

図1 ライソゾーム病の起こり方

ライソゾーム病は当該酵素をコードする遺伝子に変異が起こり、そのため酵素活性が低下する。その結果、当該酵素の基質が蓄積し、細胞レベル・組織レベルの異常が起き臨床症状が現れる。

である。蓄積する物質の性状および罹患臓器により種々の症状を呈する。リビドーシスは中枢神経症状を、MPSは粗な顔貌、骨変形、関節拘縮を、糖原病は筋力低下を主症状とする。神経学的退行を示した場合、肝脾腫・脱髄・瘻性の有無や眼底所見に留意して鑑別診断を考える。表1に主なライソゾーム病の主要症状と

鑑別診断をまとめる。診断は臨床症状から考えられる疾患を推察し、白血球あるいは培養皮膚線維芽細胞の酵素活性測定によって確定診断される。

### 3 治療の実際

現在、わが国で確立している治療は造血幹細胞移植と酵素補充療法である。前者についてはMPS I型、MPS II型、副腎白質変性症が主な対象疾患である。後者の対象疾患はゴーシェ(Gaucher)病、ファブリ(Fabry)病、MPS I型、MPS II型、MPS VI型、ポンペ病の6疾患のみである。

**看護のポイント** .....  
難治性かつ慢性疾患なので家族の心理的負担を緩和するような心理的支援を視野に入れた看護が重要である。(井田博幸)

表1 ライソゾーム病の主な臨床症状と鑑別診断

		有	ゴーシェ病2型/3型
		肝脾腫	無
神経学的退行	脱髄	有	クラッベ病、異染性白質変性症、副腎白質変性症
		無	ゴーシェ病2型/3型、GM2 ガングリオシドーシス、GM1 ガングリオシドーシス
	瘻性	有	クラッベ病、異染性白質変性症、副腎白質変性症、ゴーシェ病2型/3型
		無	GM2 ガングリオシドーシス
眼所見	チェリーレッドスポット	GM1 ガングリオシドーシス、GM2 ガングリオシドーシス	
	網膜色素変性	セロイドリポフスチン症	
	角膜混濁	MPS I型	
皮膚所見	被角血管腫	ファブリ病、フコシドーシス、ガラクトシアリドーシス、マンノシドーシス	
	魚鱗癬	マルチプルスルファターゼ欠損症	
	皮下結節	ファーバー病	
粗大骨端	骨・関節変化	重度	MPS I型、MPS II型、MPS IV型、MPS VI型
		軽度	MPS III、GM1 ガングリオシドーシス、I-cell病、フコシドーシス、マンノシドーシス、マルチプルスルファターゼ欠損症
筋緊張低下			ポンペ病
肝脾腫(神経症状なし)			ゴーシェ病1型

## 先天性甲状腺機能低下症(クレチン症)

congenital hypothyroidism (cretinism)

### 1 起こり方

胎児期あるいは周産期に生じた甲状腺ホルモンの作用不全に起因する。障害の部位により視床下部(3次性)、下垂体(2次性)および甲状腺(原発性)に分類されるが、甲状腺の障害(甲状腺の形成異常や甲状腺ホルモン合成障害など)が90%以上を占める。したがって血中甲状腺刺激ホルモン(TSH)の上昇を指標に新生児マススクリーニング(MS)が施行されている。頻度は、約3,000~4,000人に1人と推計されている。

### 2 症状と診断のすすめ方

#### 症 状

大部分の症例がMSで見出されるため、新生児期の症状がもっとも重要で、その症状は①代謝低下(遷延性黄疸、便秘、臍ヘルニア、体重増加不良、皮膚乾燥、不活発、四肢冷感)、②浮腫(巨舌、嚔声、浮腫)および骨発育の遅延(小泉門開大)による。甲状腺腫を認める症例もある(ヨード不足やホルモン合成障害でみられ、甲状腺腫性クレチン症とよばれる)。これらの症状はチェックリストの観察項目で、多いほど重症で、2つ以上症状がある場合はただちに治療を開始する。未治療で経過している重症クレチン症では、特有な顔貌(腫れぼったい眼瞼、巨舌、鞍鼻など)を呈し、低身長や運動発達遅延などをきたす。このような症例は今日きわめてまれである。

#### 診断のすすめ方

MSの初回濾紙血でTSH値が15~30μU/mL以上(濾紙血は全血のため、血清表示ではその1.6倍の値に相当する)の場合はただちに医療機関で精密検査を行う。上記の値未満で10μU/mL以上は再び濾紙血検査を行い、再度10μU/mL以上であれば精密検査を行う。

早産児では間脳下垂体のフィードバック機構が未熟なため、本症でもTSHの上昇が不十分なことがある。2,000g以下で出生した児では、生後1ヵ月あるいは2,500gに達した時点で2回目のMSを行う。

精密検査では、血中TSH上昇を確認するとともに、遊離T<sub>3</sub>、遊離T<sub>4</sub>を測定する。甲状腺機能低下状態では、最初に遊離T<sub>4</sub>値の低下が認められるため、診断には遊離T<sub>4</sub>の低下が重要である。骨発育の指標として大腿骨遠位骨端核X線検査を行う。大腿骨遠位部の骨端核は、成熟児は出生時から出現している。本症では骨端核が出現していないか、あるいは出現していても小さく、重症度の目安となる。血清サイログロブリンは甲状腺無形成では感度以下、有機化障害では高値を示すことが多く原因検索に役立つ。超音波検査で甲状腺が描出されない(無形成、異所性甲状腺)あるいは小さい(低形成)の場合、本症の確定診断に役立つ。鑑別に重要なものとして、乳児一過性高TSH血症(血清TSHが高値であるが、①血中甲状腺ホルモン値が常に正常範囲内、②乳児期にTSHが正常化する、③甲状腺機能低下を引き起こす原因がない、④甲状腺エコーやシンチグラムに異常がない)、新生児一過性甲状腺機能低下症[母体への抗甲状腺薬投与、阻害型TSH受容体抗体(TBII)、胎児造影、母体や新生児へのヨード大量曝露などが原因となり、治療の対象となる]がある。

### 3 治療の実際

治療はレボチロキシン(T<sub>4</sub>)を用い、10μg/kg/日(重症の場合は15μg/kg/日)で開始し、TSH値を正常域に、遊離T<sub>4</sub>値を正常上限に保つよう調節する。チェックリストで2項目以上の症状、大腿骨遠位骨端核出現の遅れ、MS濾紙血TSH高値(初回濾紙血でTSH値が30μU/mL

Case report

## An adult patient with mucopolipidosis III alpha/beta presenting with parkinsonism

Munetsugu Hara<sup>a</sup>, Takahiro Inokuchi<sup>b</sup>, Takayuki Taniwaki<sup>c</sup>, Takanobu Otomo<sup>d</sup>,  
Norio Sakai<sup>d</sup>, Toyojiro Matsuishi<sup>a</sup>, Makoto Yoshino<sup>a,\*</sup>

<sup>a</sup> Department of Pediatrics & Child Health, Department of Medicine, Kurume University School of Medicine, 67 Asahi-machi, Kurume, Fukuoka 830-0011, Japan

<sup>b</sup> Research Institute of Medical Mass Spectrometry, Kurume University School of Medicine, 67 Asahi-machi, Kurume, Fukuoka 830-0011, Japan

<sup>c</sup> Division of Respiriology, Neurology, and Rheumatology, Department of Medicine, Kurume University School of Medicine, 67 Asahi-machi, Kurume, Fukuoka 830-0011, Japan

<sup>d</sup> Department of Developmental Medicine (Pediatrics) D-5, Osaka University Graduate School of Medicine, 2-2 Yamadaoka, Suita, Osaka 565-0871, Japan

Received 14 October 2011; received in revised form 11 June 2012; accepted 14 July 2012

### Abstract

A 36-year-old man with mucopolipidosis type III alpha/beta presented with hypoactivity, mutism, muscle rigidity, and involuntary movement. The involuntary movement was interpreted to be tremor at rest on physical examination and surface electromyography, which revealed mostly asynchronous contractions at 3–4 Hz of the biceps and triceps brachii muscles. All these symptoms were consistent with abnormalities of parkinsonism, which is caused by an insult to the basal ganglia that permeates the entire basal ganglia-thalamocortical circuitry. This report is the first to present a case of mucopolipidosis type III alpha/beta in association with parkinsonism.

© 2012 The Japanese Society of Child Neurology. Published by Elsevier B.V. All rights reserved.

**Keywords:** Mucopolipidosis type III alpha/beta; N-acetylglucosamine-1-phosphate transferase, alpha and beta subunits; Tremor at rest; Surface electromyography; Parkinsonism; The basal gangliathalamocortical circuitry

### 1. Introduction

Mucopolipidosis type II (ML II), or I-cell disease (OMIM #252500), and its attenuated form ML III alpha/beta (OMIM #252600) are allelic diseases caused by a congenital deficiency of the UDP-*N*-acetylglucosa-

mine: lysosomal enzyme *N*-acetylglucosamine phosphotransferase (E.C. 2.7.8.17) [1,2]. Deficiency of this enzyme results in failure of multiple lysosomal enzymes to be localized in the lysosomal compartment, where they normally hydrolyze substrates [3].

Typical symptoms are skeletal dysplasia, stiffness of the joints, claw hand deformity, short stature, scoliosis, mild coarsening of the face, corneal clouding, mild retinopathy, astigmatism, and cardiac valve involvement [2,4]. In contrast to these conspicuous extraneural symptoms however, neurological signs and symptoms are relatively limited: learning disability or mental retardation has been reported in nearly 50% of patients, and carpal tunnel syndrome is a common complication [4,5]. Other

*Abbreviations:* GNPTAB, N-acetylglucosamine-1-phosphate transferase, alpha and beta subunits; GNPTG, N-acetylglucosamine-1-phosphate transferase, gamma subunit; ML III alpha/beta, mucopolipidosis type III alpha/beta; ML II, mucopolipidosis type II; MRI, magnetic resonance imaging

\* Corresponding author.

E-mail address: yoshino\_m@space.ocn.ne.jp (M. Yoshino).

neurological signs are barely encountered [6]. The association of involuntary movements with ML III has not been described previously.

## 2. Case report

A 36-year-old man was referred to our department for management of pain in the hands. His perinatal history was noncontributory. By 18 months of age, he presented with coarse face, mild joint contracture of the hands, and short stature, and later presented with bilateral dislocation of the hip at age 1 year 10 months and aortic regurgitation at age 13 years. At around 16 years of age, he began to develop fine trembling of the left arm, which became prominent by age 20. At age 23, he became hypoactive and mutistic. Around age 24, he began to develop rhythmic movements of the head and bilateral arms, hands, and legs, induced by motion or mental strain, for which clonazepam was prescribed. At age 29, he developed pain in the tips of the fingers and toes. There was no family history of neurological disorders or involuntary movements.

Physical examination revealed a man with short stature, macroglossia, thick lips, thoracolumbar kyphosis, a short and narrow thoracic cage, abdominal protuberance, hepatosplenomegaly, umbilical hernia, and bilateral clubfeet. His height was 99.3 cm and weight 24.6 kg. Breath sound was vesicular. A grade II/VI regurgitant murmur was audible over the right second intercostal space parasternally and in Erb's area. He was alert and responded appropriately to questions, although he was generally taciturn. His full intelligence quotient was 52 (verbal, 60; performance, 54) on the Wechsler Intelligence Scale for Children-III. Cranial nervous system was intact, and eye movements were not restricted. Deep tendon reflexes were generally exaggerated; more so in the lower extremities than in the upper extremities. Muscle power was decreased. Muscle tone was slightly increased with minimum cogwheel rigidity, although joint contracture obscured partly evaluation of these findings. His movements were slow. There was no intention tremor. He had thermalgia and hyperesthesia confined to distal portions of wrist joints, but tactile and thermal sensations were intact in both upper limbs.

He had rhythmic movements with a frequency of 3–4 Hz of the head with yes–yes type and extremities that persisted for several minutes during the daytime. This was often observed when the patient was at rest and disappeared at bedtime, and could be evoked proactively and reactively as well as occasionally by mental strain, but was not associated with dystonic movements and not affected by postural change.

Diagnosis of ML III alpha/beta was confirmed from reduced  $\beta$ -galactosidase activity in lymphocytes, and increased activity of  $\beta$ -galactosidase,  $\beta$ -hexosaminidase,

$\alpha$ -mannosidase, and  $\alpha$ -fucosidase in serum. Mutational analysis of *GNPTAB* revealed compound heterozygosity for one nonsense mutation, c.3565C>T (p.R1189X), and one missense mutation, c.1120C>T (p.F374L).

Surface electromyography was recorded from the biceps and triceps brachii muscles while the patient was lying on a bed. When the patient was at rest without any voluntary posture or movement, the frequency of the waves was about 3–4 Hz (Fig. 1). The activity of these muscles remained mostly nonsynchronous throughout the examination. No abnormal activity was elicited in the muscles of the lower extremities under these conditions. This involuntary movement was thus interpreted to be tremor at rest. The conduction velocities of the peripheral motor and sensory nerves were within normal ranges, thereby excluding carpal tunnel syndrome.

Single photon emission computed tomography showed decreased blood flow in the bifrontal lobe and occipital lobe (Fig. 2). MRI showed pressure on the cervical spine at the atlanto-axial level (Supplementary data, Fig. 3A), and an axial T2-weighted image showed a high intensity area in the dorsal horn (Supplementary data, Fig. 3A and B). In contrast, cranial MRI revealed no evidence of cerebral and cortical atrophy, and normal basal ganglia (Supplementary data, Fig. 4).

## 3. Discussion

The present patient has hypoactivity and tremor at rest. The combination of these symptoms is consistent with abnormalities of the basal ganglia that permeate the entire basal ganglia-thalamocortical circuitry, as typically seen in parkinsonism [7]. The decrease in bifrontal blood flow is consistent with mutism in the present patient, although it remains unclear whether or not it is linked with the disturbance in the above-mentioned circuitry.

Neuropathological study of ML III has been confined to one patient [8] and revealed moderate accumulation of lipofuscin granules in the neuronal cells of the thalamus and hypothalamus. The involvement of these areas

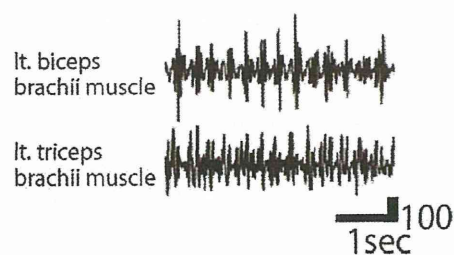


Fig. 1. Surface electromyogram recorded from the biceps and triceps brachii muscles at rest, showing asynchronous contractions of the antagonist muscles, with a frequency of 3–4 Hz.

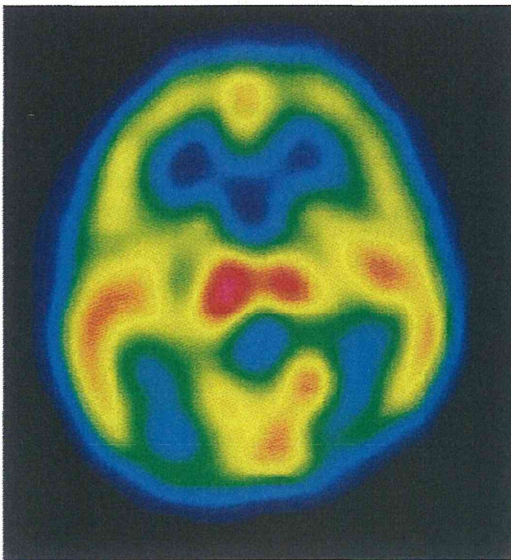


Fig. 2. Axial single photon emission computed tomography image of head shows decreased blood flow in the bifrontal lobe and occipital lobe.

might affect the basal ganglia-thalamocortical circuitry in ML II and ML III and hence might have induced the tremor in the present patient.

Several lines of evidence have shown that in cultured ML II and ML III skin fibroblasts, mitochondrial function was impaired [9]. It seems likely that a similar pathophysiological process operates in the central nervous system and the deleterious effects of such a process could be more pronounced in non-dividing cells like neurons than in dividing, cultured cells [8].

In hereditary Parkinson's disease, mitochondrial dysfunction is implicated in dopamine neuronal toxicity [10]. It is possible therefore, that impaired mitochondrial function in the basal ganglia-thalamocortical circuitry contributes to development of parkinsonism in ML III patients.

A link between mutations of glucocerebrosidase, of which deficiency causes Gaucher disease, and Parkinson disease has been postulated, and it is now known that a wide variety of lysosomal storage diseases are associated with Parkinson disease [11]. ML III may be included in these disorders.

The present patient had thermalgia and hyperesthesia of the upper limbs: such sensory disturbances are not common features of ML III. The MRI T2-weighted image showed compression of the spinal cord at the atlanto-axial level and a high intensity area in the dorsal horn, which is the input route for tactile and pain sensations. These lesions may responsible for the sensory abnormalities of the upper limbs in the present patient.

#### Author contributions

M. Hara: neurological evaluation of the patient and manuscript composition; T. Taniwaki and T. Matsuishi: neurological evaluation of the patient and interpretation of the electrophysiological studies, suggestions regarding manuscript composition; T. Otomo and N. Sakai: conduction of enzyme studies and genetic analysis; M. Yoshino: patient care, neurological evaluation of the patient, manuscript composition, corresponding author.

#### Competing interest statement

M.Y. is a recipient of a research fund from Genzyme Japan K.K. The other authors have no competing interest to declare. The authors confirm independence from the sponsor; the content of the article has not been influenced by the sponsors.

#### Patient consent

The authors confirm that patient has given consent to submit this article on the condition that the patient's privacy is securely protected.

#### Acknowledgments

This work was supported in part by grant-in-aid from the Japanese Ministry of Health, Labour and Welfare of Japan.

#### Appendix A. Supplementary data

Supplementary data associated with this article can be found, in the online version, at <http://dx.doi.org/10.1016/j.braindev.2012.07.009>.

#### References

- [1] Reitman ML, Varki A, Kornfeld S. Fibroblasts from patients with I-cell disease and pseudo-Hurler polydystrophy are deficient in uridine 5'-diphosphate-*N*-acetylglucosamine: glycoprotein *N*-acetylglucosaminylphosphotransferase activity. *J Clin Invest* 1981;67:1574–9.
- [2] Kornfeld S, Sly WS. I-cell disease and pseudo-Hurler polydystrophy: disorders of lysosomal enzyme phosphorylation and localization. In: Scriver CR, Beaudet AL, Sly WS, Valle D, editors. *The metabolic & molecular bases of inherited disease*. 8th ed, vol. 3. New York: McGraw-Hill; 2001. p. 3469–82.
- [3] Kaplan A, Fischer D, Achord D, Sly W. Phosphohexosyl recognition is a general characteristic of pinocytosis of lysosomal glycosidases by human fibroblasts. *J Clin Invest* 1977;60:1088–93.
- [4] Kelley TE, Thomas GH, Taylor Jr HA, McKusick VA, Sly WS, Glaser JH, et al. Mucopolidosis III (pseudo-Hurler polydystrophy): clinical and laboratory studies in a series of 12 patients. *Johns Hopkins Med J* 1975;137:156–75.

- [5] Smuts I, Potgieter D, van der Westhuizen FH. Combined tarsal and carpal tunnel syndrome in mucopolipidosis type III. A case study and review. *Ann N Y Acad Sci* 2009;1151:77–84.
- [6] Okada S, Owada M, Sakiyama T, Yutaka T, Ogawa M. I-cell disease: clinical studies of 21 Japanese cases. *Clin Genet* 1985;28:207–15.
- [7] Galvan A, Wichmann T. Pathophysiology of parkinsonism. *Clin Neurophysiol* 2008;119:1459–74.
- [8] Kobayashi H, Takahashi-Fujigasaki J, Fukuda T, Sakurai K, Shimada Y, Nomura K, et al. Pathology of the first autopsy case diagnosed as mucopolipidosis type III  $\alpha/\beta$  suggesting autophagic dysfunction. *Mol Genet Metab* 2011;102:170–5.
- [9] Otomo T, Higaki K, Nanba E, Ozono K, Sakai N. Inhibition of autophagosome formation restores mitochondrial function in mucopolipidosis II and III skin fibroblasts. *Mol Genet Metab* 2009;98:393–9.
- [10] Pan T, Kondo S, Le W, Jankovic J. The role of autophagy–lysosome pathway in neurodegeneration associated with Parkinson’s disease. *Brain* 2008;131:1969–78.
- [11] Shachar T, Bianco CL, Recchia A, Wiessner C, Raas-Rothschild A, Futerman AH. Lysosomal storage disorders and parkinson’s disease: Gaucher disease and beyond. *Mov Disord* 2011;26:1593–604.

Case report

# Isolated pyramidal tract impairment in the central nervous system of adult-onset Krabbe disease with novel mutations in the *GALC* gene

Shin-ichi Tokushige<sup>a,\*</sup>, Tomohiro Sonoo<sup>a</sup>, Risa Maekawa<sup>a</sup>, Yuichiro Shirota<sup>b</sup>,  
Ritsuko Hanajima<sup>b</sup>, Yasuo Terao<sup>b</sup>, Hideyuki Matsumoto<sup>b</sup>, Mohammad Arif Hossain<sup>c</sup>,  
Norio Sakai<sup>c</sup>, Yasushi Shiio<sup>a</sup>

<sup>a</sup> Department of Neurology, Tokyo Teishin Hospital, 2-14-23 Fujimi, Chiyoda-ku, Tokyo 102-8798, Japan

<sup>b</sup> Department of Neurology, Graduate School of Medicine, Faculty of Medicine, The University of Tokyo, Japan

<sup>c</sup> Department of Pediatrics, Osaka University Graduate School of Medicine, Japan

Received 11 May 2012; received in revised form 8 August 2012; accepted 8 August 2012

## Abstract

This report describes a 60-year-old female patient with Krabbe disease who presented with slowly progressive gait disturbance due to mild spastic paraplegia. Brain magnetic resonance imaging showed high-intensity lesions along the upper parts of the bilateral pyramidal tracts in fluid-attenuated inversion recovery images. Central motor conduction time was prolonged both in the upper and the lower extremities, while central sensory conduction time was normal. The reduced lymphocyte galactocerebrosidase (*GALC*) activity and two novel mutations in the *GALC* gene, p.G496S and p.G569S, proved the diagnosis of Krabbe disease. Our findings show that adult-onset Krabbe disease is characterized by isolated pyramidal tract impairment in the central nervous system, both neurophysiologically and radiologically.

© 2012 The Japanese Society of Child Neurology. Published by Elsevier B.V. All rights reserved.

**Keywords:** Krabbe disease; Magnetic resonance imaging (MRI); Motor evoked potential (MEP); Pyramidal tract; Galactocerebrosidase (*GALC*)

## 1. Introduction

Krabbe disease is an autosomal recessive lysosomal storage disease caused by loss of galactocerebrosidase (*GALC*) activity [1]. Patients with adult-onset Krabbe disease typically develop slowly progressive spastic paraplegia and sometimes sensorimotor neuropathy [1,2]. Although magnetic resonance imaging (MRI) revealed that the involvement of pyramidal tracts is characteristic of adult-onset Krabbe disease [3,4], there have been few reports on neurophysiology of the pyramidal tracts [5]. Here, we present a case of adult-onset Krabbe disease

with novel mutations of the *GALC* gene. Neurophysiological studies revealed delayed central motor conduction with normal central sensory conduction, in accordance with the MRI findings.

## 2. Case report

A 60-year-old Japanese woman who had experienced slowly progressive gait disturbance was referred to our hospital. Her past medical history and family history were unremarkable. She had no siblings and her parents were non-consanguineous. Neurological examination revealed mild spastic paraplegia, exaggerated patellar tendon reflexes, and positive Babinski and Chaddock reflexes. She exhibited no cognitive dysfunction, sensory loss, ataxia, or autonomic dysfunction.

\* Corresponding author. Tel.: +81 3 5214 7111.  
E-mail address: tokushige-ky@umin.ac.jp (S. Tokushige).

Brain MRI revealed high-intensity lesions along the upper parts of the bilateral pyramidal tracts in fluid-attenuated inversion recovery (FLAIR) images (Fig. 1). Nerve conduction studies (NCS) showed decreased motor and sensory conduction velocities. A sensory evoked potential (SEP) study revealed normal central sensory conduction time (CSCT) and delayed peripheral latencies. Motor evoked potentials (MEPs) were recorded from the left first dorsal interosseous (FDI) and tibialis anterior (TA) muscles using the method reported by Matsumoto et al. [6,7] and Ugawa et al. [8]. As shown in Table 1, the central motor conduction time (CMCT) was prolonged, especially between the cortex and the brainstem. The cortico-conus motor conduction time (CCCT), which is the most direct indicator of pyramidal tract conduction [6], was also prolonged. Needle electromyography in the biceps brachii, flexor carpi ulnaris, rectus femoris, and tibialis anterior muscles showed reduced recruitment of motor unit potentials during voluntary contraction without any spontaneous activities during relaxation. Auditory brainstem responses, visual evoked potentials, and electroencephalography revealed no abnormalities.

Since the activity of lymphocyte GALC was reduced to 0.03 nmol/h/mg (normal range,  $2.1 \pm 0.29$  nmol/h/mg [9]), the patient received a diagnosis of Krabbe disease. We investigated the DNA sequence for all 17 exons of the *GALC* gene, and found two novel heterozygous missense mutations, p.G496S and p.G569S (Fig. 2A and B), which were not found in 100 healthy controls.

### 3. Discussion

We described a case of adult-onset Krabbe disease with slowly progressive gait disturbance due to mild spastic paraplegia. Brain MRI showed bilateral lesions along the upper pyramidal tracts, and neurophysiological studies revealed delayed central motor conduction with normal central sensory conduction. The lymphocyte GALC activity was decreased and two heterozygous mutations were found in the *GALC* gene, which proved the diagnosis of Krabbe disease.

Matsumoto et al. [5] reported a 30-year-old female patient with Krabbe disease with severe spastic paraplegia, whose CMCT was prolonged and CSCT was normal, in a pattern identical to that seen in our patient. Therefore, isolated pyramidal tract impairment appears to be a common feature of adult-onset Krabbe disease in both neurophysiological and radiological examinations. In contrast, in regard to infantile-onset Krabbe disease, a 23-month-old female patient with delayed central sensory conduction has been reported [10]. A comparison of our case with this case suggests that isolated pyramidal tract impairment may be characteristic of the adult-onset subtype or mild form of Krabbe disease.

To date, genetic studies on patients with Krabbe disease have suggested some correlation between the genotype and the clinical severity [9]. Although further analysis is needed to verify the significance of the *GALC* mutations found in our patient, the mild neurological symptoms may be related to the genotype.

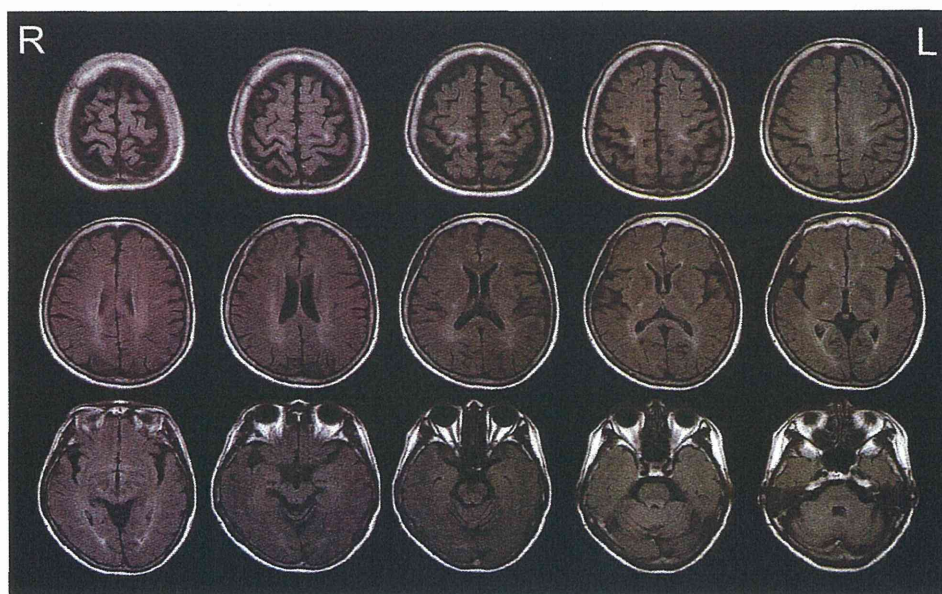


Fig. 1. FLAIR MR images of the brain showing high-intensity lesions along the upper part of the bilateral pyramidal tracts from just beneath the motor cortex to the cerebral peduncle.

Table 1  
Motor evoked potentials.

	Latency (ms)			Conduction time (ms)		
	Cortical	Brainstem	Cervical	Cortical–brainstem	Brainstem–cervical	Cortical–cervical (CMCT)
Left FDI	<b>31.3</b>	<b>23.6</b>	<b>19.3</b>	<b>7.7</b>	4.3	<b>12.0</b>
Normal range (mean ± SD)	20.7 ± 1.0	17.3 ± 0.8	13.6 ± 0.8	3.3 ± 0.3	3.7 ± 0.5	7.0 ± 0.4
	Latency (ms)		Conduction time (ms)			
	Cortical	Conus	Cortico-conus (CCCT)			
Left TA	<b>38.9</b>	<b>22.8</b>	<b>16.1</b>			
Normal range (mean ± SD)	26.1 ± 1.6	14.0 ± 1.4	12.3 ± 1.2			

FDI, first dorsal interosseous; TA, tibialis anterior; CMCT, central motor conduction time; CCCT, cortico-conus motor conduction time. Abnormal values: bold italic.

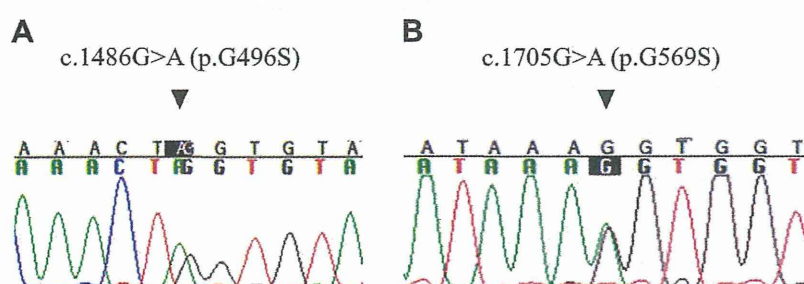


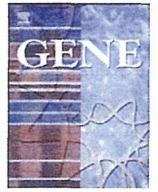
Fig. 2. Two novel missense mutations in the *GALC* gene of the patient. (A) c.1486G>A (p.G496S), (B) c.1705G>A (p.G569S).

The characteristic upper pyramidal tract lesions and decreased sensorimotor nerve conduction velocities strongly suggested the diagnosis of Krabbe disease, which was finally confirmed by the decreased *GALC* activity. Other leukodystrophies including adrenoleukodystrophy, metachromatic leukodystrophy, Pelizaeus–Merzbacher disease, Sjögren–Larsson syndrome and vanishing white matter disease were ruled out by the clinical and radiological findings.

In conclusion, the pyramidal tract is considered to be the only tract involved in the central nervous system of adult-onset Krabbe disease. Physiological and radiological studies provide consistent results on this issue.

## References

- [1] Suzuki K. Globoid cell leukodystrophy (Krabbe's disease): update. *J Child Neurol* 2003;18:595–603.
- [2] Henderson RD, MacMillan JC, Bradfield JM. Adult onset Krabbe disease may mimic motor neurone disease. *J Clin Neurosci* 2003;10:638–9.
- [3] Wang C, Melberg A, Weis J, Månsson JE, Raininko R. The earliest MR imaging and proton MR spectroscopy abnormalities in adult-onset Krabbe disease. *Acta Neurol Scand* 2007;116:268–72.
- [4] De Stefano N, Dotti MT, Mortilla M, Pappagallo E, Luzi P, Rafi MA, et al. Evidence of diffuse brain pathology and unspecific genetic characterization in a patient with an atypical form of adult-onset Krabbe disease. *J Neurol* 2000;247:226–8.
- [5] Matsumoto R, Kohara N, Kaji R, Fukuyama H, Shibasaki H, Kimura J. Electrophysiological studies of adult type Krabbe's disease. *Electroencephalogr Clin Neurophysiol* 1995;95:P91–2.
- [6] Matsumoto H, Hanajima R, Shirota Y, Hamada M, Terao Y, Ohminami S, et al. Cortico-conus motor conduction time (CCCT) for leg muscles. *Clin Neurophysiol* 2010;121:1930–3.
- [7] Matsumoto H, Hanajima R, Terao Y, Hamada M, Yugeta A, Shirota Y, et al. Efferent and afferent evoked potentials in patients with adrenomyeloneuropathy. *Clin Neurol Neurosurg* 2010;112:131–6.
- [8] Ugawa Y, Uesaka Y, Terao Y, Hanajima R, Kanazawa I. Magnetic stimulation of corticospinal pathways at the foramen magnum level in humans. *Ann Neurol* 1994;36:618–24.
- [9] Xu C, Sakai N, Taniike M, Inui K, Ozono K. Six novel mutations detected in the *GALC* gene in 17 Japanese patients with Krabbe disease, and new genotype-phenotype correlation. *J Hum Genet* 2006;51:548–54.
- [10] Kurokawa T, Chen YJ, Nagata M, Hasuo K, Kobayashi T, Kitaguchi T. Late infantile Krabbe leukodystrophy: MRI and evoked potentials in a Japanese girl. *Neuropediatrics* 1987;18:182–3.



## Short Communication

## 14-3-3ε Gene variants in a Japanese patient with left ventricular noncompaction and hypoplasia of the corpus callosum

Bo Chang <sup>a,e</sup>, Carlos Gorbea <sup>b</sup>, George Lezin <sup>b</sup>, Ling Li <sup>b</sup>, Lishen Shan <sup>a,e</sup>, Norio Sakai <sup>c</sup>, Shigetoyo Kogaki <sup>c</sup>, Takano Otomo <sup>c</sup>, Takeshi Okinaga <sup>c</sup>, Akiko Hamaoka <sup>d</sup>, Xianyi Yu <sup>e</sup>, Yukiko Hata <sup>f</sup>, Naoki Nishida <sup>f</sup>, H. Joseph Yost <sup>g</sup>, Neil E. Bowles <sup>b</sup>, Luca Brunelli <sup>b,\*</sup>, Fukiko Ichida <sup>a,\*\*</sup>

<sup>a</sup> Department of Pediatrics, University of Toyama, Toyama, Japan

<sup>b</sup> Department of Pediatrics, University of Utah School of Medicine, Salt Lake City, USA

<sup>c</sup> Department of Pediatrics, Osaka University Graduate School of Medicine, Osaka, Japan

<sup>d</sup> Department of Pediatrics, Kyoto Medical School, Kyoto, Japan

<sup>e</sup> Department of Pediatrics, the Shengjing Hospital affiliated to China Medical University, Shenyang, China

<sup>f</sup> Department of Legal Medicine, University of Toyama, Toyama, Japan

<sup>g</sup> Department of Neurobiology and Anatomy, University of Utah School of Medicine, Salt Lake City, USA

## ARTICLE INFO

## Article history:

Accepted 2 December 2012

Available online 20 December 2012

## Keywords:

Ventricular noncompaction

14-3-3 proteins

YWHAE variants

Myocardial morphogenesis

Cardiomyopathy

Brain development

## ABSTRACT

**Background:** Left ventricular noncompaction (LVNC) is a cardiomyopathy characterized by a prominent trabecular meshwork and deep intertrabecular recesses, and is thought to be due to an arrest of normal endomyocardial morphogenesis. However, the genes contributing to this process remain poorly understood. 14-3-3ε, encoded by *YWHAE*, is an adapter protein belonging to the 14-3-3 protein family which plays important roles in neuronal development and is involved in Miller–Dieker syndrome. We recently showed that mice lacking this gene develop LVNC. Therefore, we hypothesized that variants in *YWHAE* may contribute to the pathophysiology of LVNC in humans.

**Methods and results:** In 77 Japanese patients with LVNC, including the probands of 29 families, mutation analysis of *YWHAE* by direct DNA sequencing identified 7 novel variants. One of them, c.–458G>T, in the *YWHAE* promoter, was identified in a familial patient with LVNC and hypoplasia of the corpus callosum. The –458G>T variant is located within a regulatory CCAAT/enhancer binding protein (C/EBP) response element of the *YWHAE* promoter, and it reduced promoter activity by approximately 50%. Increased binding of an inhibitory C/EBP3 isoform was implicated in decreasing *YWHAE* promoter activity. Interestingly, we had previously shown that C/EBP3 is a key regulator of *YWHAE*.

**Conclusions:** These data suggest that the –458G>T *YWHAE* variant contributes to the abnormal myocardial morphogenesis characteristic of LVNC as well as abnormal brain development, and implicate *YWHAE* as a novel candidate gene in pediatric cardiomyopathies.

© 2012 Elsevier B.V. All rights reserved.

### 1. Introduction

Left ventricular noncompaction (LVNC) is a cardiomyopathy morphologically characterized by a 2-layered myocardium, numerous prominent trabeculations, and deep intertrabecular recesses communicating with the left ventricular cavity (Chin et al., 1990; Jenni et al., 1999;

Oechslin et al., 2000). Increased awareness and the use of modern ultrasound technology have resulted in increased detection of the morphological features of LVNC in routine clinical practice (Ichida et al., 1999; Jenni et al., 2007; Pignatelli et al., 2003; Stollberger et al., 2002).

LVNC has been classified as a primary cardiomyopathy with a genetic origin (Maron et al., 2006). The clinical manifestations of LVNC are highly variable, ranging from no symptoms to a progressive deterioration in cardiac function resulting in congestive heart failure, arrhythmias, thromboembolic events, and sudden cardiac death (Chin et al., 1990; Ichida et al., 1999; Jenni et al., 1999; Pignatelli et al., 2003; Ritter et al., 1997). The mechanism of LVNC is widely believed to be an arrest of myocardial morphogenesis during embryogenesis (Bartram et al., 2007; Chin et al., 1990; Dusek et al., 1975). Up to 40% of LVNC patients have evidence of familial disease, based on clinical assessment of the family members of probands, and there is significant genetic heterogeneity in this disorder (Ichida et al., 1999).

**Abbreviations:** LVNC, Left ventricular noncompaction; ECG, electrocardiogram; PCR, polymerase chain reaction; ESE, exonic splice enhancer; LAP\*, full-length liver-activating protein; LAP, medium-length liver-activating protein; LIP, liver-inhibitory protein.

\* Correspondence to: L. Brunelli, Department of Pediatrics, University of Utah School of Medicine, E1HC, 15 North 2030 East, Rm 3290, Salt Lake City, UT, 84112, USA. Tel.: +1 801 587 3498; fax: +1 801 585 5470.

\*\* Correspondence to: F. Ichida, Department of Pediatrics, University of Toyama, 2630 Sugitani, Toyama 930-0194, Japan. Tel.: +81 76 434 7311; fax: +81 76 434 5029.

E-mail addresses: [luca.brunelli@genetics.utah.edu](mailto:luca.brunelli@genetics.utah.edu) (L. Brunelli), [fukiko@med.u-toyama.ac.jp](mailto:fukiko@med.u-toyama.ac.jp) (F. Ichida).

In children, X-linked, autosomal dominant and mitochondrial inheritance has been reported, while in adults autosomal dominant inheritance has been described (Sasse-Klaassen et al., 2003).

In recent years, genetic heterogeneity has been demonstrated in most of the inherited cardiovascular diseases, including the long QT syndromes, dilated cardiomyopathy, and hypertrophic cardiomyopathy. To date, variations in several genes have been reported in patients with LVNC, including *DTNA*, *TAZ*, *LMNA*, *MYH7*, *ACTA*, *TNNT2*, *LDB3* and *SCN5A* (Chen et al., 2002; Hermida-Prieto et al., 2004; Ichida et al., 2001; Klaassen et al., 2008; Shan et al., 2008; Vatta et al., 2003; Xing et al., 2006). However, the relatively small contribution of known mutations to the disease, compared to the higher proportion of familial cases suggests that other elusive genes remain to be identified.

14-3-3 $\epsilon$ , encoded by *YWHAE*, is a scaffold adapter protein belonging to the 14-3-3 protein family, which binds phosphoserine/threonine residues (Aitken et al., 1992; Fu et al., 2006; Muslin et al., 1996; Yaffe et al., 1997). 14-3-3 proteins work as regulatory proteins that interact with other proteins in a phosphorylation dependent or independent manner (Han et al., 2001). They consist of at least seven mammalian isoforms, namely  $\beta$ ,  $\gamma$ ,  $\epsilon$ ,  $\eta$ ,  $\zeta$ ,  $\sigma$ , and  $\tau/\theta$ , each encoded by a distinct gene. They are ubiquitously expressed and highly conserved, with a subunit mass of ~28–33 kDa (Aitken et al., 1992; Fu et al., 2006; Tzivion et al., 2001; Wilker and Yaffe, 2004). 14-3-3 $\epsilon$  has been shown to play important roles in neuronal development and is involved in Miller–Dieker syndrome, as well as in periventricular heterotopias and marked corpus callosum hypoplasia (Aitken et al., 1992; Mignon-Ravix et al., 2010; Toyo-oka et al., 2003). 14-3-3 proteins and 14-3-3 $\epsilon$  have also been shown to play important roles in cardiac channel activity both *in vitro* and *in vivo* (Allouis et al., 2006; Choe et al., 2006; Kagan et al., 2002; Zhang et al., 2003). We have recently shown that mice lacking *Ywhae* display a cardiac morphology consistent with an LVNC phenotype (Kosaka et al., in press). Most of these mice also have ventricular septal defects, a structural abnormality commonly associated with LVNC in humans (Kosaka et al., in press). Based on these data, we hypothesized that *YWHAE* could be a candidate gene for LVNC in humans.

## 2. Materials and methods

### 2.1. Subjects

Blood was obtained from 77 Japanese patients including 29 familial cases (12 females and 17 males) and 48 sporadic cases (15 females and 33 males), after informed consent, and then genomic DNA was extracted using QuickGene DNA whole blood kits (FUJIFILM; JAPAN). Two hundred ethnicity-matched normal controls were recruited and DNA was extracted in an identical manner after informed consent. The study was approved by the Research Ethics Committee of Toyama University Hospital.

### 2.2. Clinical diagnostic criteria

The diagnosis of LVNC was made by echocardiography on the basis of the following criteria established by Ichida et al. (2001), including: (1) LV hypertrophy with deep endomyocardial trabeculations in  $\geq 1$  ventricular wall segments, (2) reduced LV systolic function, (3) a two-layered endocardium with a noncompacted to compacted ratio of  $>2.0$ , and (4) deep recesses filled with blood from the ventricular cavity visualized on color Doppler imaging.

The clinical evaluation of the proband included physical examination while echocardiography (2D, M-mode, and color Doppler) was used to evaluate the cardiac structure, LV size and function (shortening fraction and ejection fraction), and valve regurgitation. At the same time, chest radiography, electrocardiography, and a complete blood count with differential were performed. Once a proband was identified, a family history was obtained, and all potentially informative family

members underwent physical examination, chest radiograph, electrocardiogram (ECG), and echocardiogram.

### 2.3. Molecular genetic studies

The 6 coding exons of *YWHAE*, including 832 nucleotides of the promoter, were amplified by polymerase chain reaction (PCR) using primers designed using the “ExonPrimer” utility through the UCSC Genome Bioinformatics Site (<http://genome.ucsc.edu>) (Table 1). PCR reactions were performed in a 25  $\mu$ l volume containing 2.5  $\mu$ l 2 mM dNTP mixture (Takara Bio, Japan), 5  $\mu$ l 5 $\times$  buffer, 1.5  $\mu$ l 25 mM MgCl<sub>2</sub>, 1.25  $\mu$ l 5 mM of each primer, 100 ng genomic DNA and 1.25 U *Taq* DNA polymerase (Promega, Madison, WI, USA). PCR amplification was performed in a Peltier Thermal Cycler using the following conditions: a 3 min denaturation step at 95 °C, 45 cycles of amplification (95 °C for 30 s, X °C for 30 s, and 72 °C for 45 s: X is the annealing temperature shown in Table 1), and a final incubation at 72 °C for 3 min. After PCR amplification, the samples were purified, directly sequenced and analyzed according to the ABI Big Dye Terminator Cycle Sequencing protocol and an ABI 310 Automated Sequencer (Applied Biosystems; Foster City, CA, USA). Blast search analysis was used to identify homology between the sequences obtained from patients and the published gene sequences. Variants were confirmed by repeating the PCR from the genomic DNA template and sequencing the PCR products. When a putative mutation was identified, the family members of the proband and at least 200 control chromosomes were screened for the sequence variations to recognize common polymorphisms.

### 2.4. Generation of the $-458G>T$ *YWHAE* promoter variant reporter

Cloning of the human *YWHAE* promoter and generation of the pGL3-Basic plasmid DNA expressing firefly luciferase under the control of *YWHAE* promoter (*YWHAE*-pGL3) were described previously (Brunelli et al., 2007). A mutated human *YWHAE* promoter containing the  $-458G>T$  variant was prepared using the QuikChange II Site-Directed Mutagenesis Kit (Stratagene, Santa Clara, CA, USA) according to the protocol of the manufacturer. The wild type plasmid DNA was PCR amplified with site-directed mutated primers (5'-GAA GCC TCA GAT TTC GGT AAA GAA GAC CTG CCA TG-3' and 5'-CAT GGC AGG TCT TCT TTA CCG AAA TCT GAG GCT TC-3'). The mutated fragment was subcloned into pGL3-Basic (*M-YWHAE*-pGL3), and confirmed by DNA sequencing.

### 2.5. Transient transfection and luciferase assay

Spontaneously transformed human umbilical vein endothelial cells (ECV-304) were prepared as previously described (Brunelli et al., 2007). Briefly, cells were seeded at 50–60% confluence in a 35 mm tissue culture dish and cultured in high glucose DMEM containing L-glutamine, sodium pyruvate and 10% FBS. ECV-304 at 60% confluence were co-transfected with either 1  $\mu$ g of *YWHAE*-pGL3 or *M-YWHAE*-pGL3, and 10 ng of phRL-CMV Renilla luciferase reporter vector using 3  $\mu$ l of FuGENE 6 per 35 mm tissue culture dish for 8 h, and the luciferase activity of *YWHAE*-pGL3 and *M-YWHAE*-pGL3 was determined as previously described (Brunelli et al., 2007). Each bar reported in the promoter activity figure is the mean  $\pm$  SD of at least three experiments.

### 2.6. Nuclear extract preparation and streptavidin-agarose pull down assay

Nuclear extracts were prepared as previously described (Brunelli et al., 2007). Binding of nuclear proteins to biotinylated probes was assayed by streptavidin pull down as previously described (Brunelli et al., 2007). Briefly, 100 or 200  $\mu$ g nuclear extract proteins were incubated with a mixture of 4  $\mu$ g of double-stranded biotinylated oligonucleotides,